INCREMENTS IN AEROFOIL LIFT COEFFICIENT AT ZERO ANGLE OF ATTACK AND IN MAXIMUM LIFT COEFFICIENT DUE TO DEPLOYMENT OF A SINGLE-SLOTTED TRAILING-EDGE FLAP, WITH OR WITHOUT A LEADING-EDGE HIGH-LIFT DEVICE, AT LOW SPEEDS

1. NOTATION AND UNITS

		SI	*British*
$(a_1)_0$	basic aerofoil lift-curve slope in incompressible flow	rad^{-1}	rad^{-1}
C_{Lm}	maximum lift coefficient of aerofoil with high-lift devices deployed, based on c		
$(C_{LmB})_d$	maximum lift coefficient of basic aerofoil at datum Reynolds number $R_c = 3.5 \times 10^6$		
C_{L0}	lift coefficient at zero angle of attack for aerofoil with high-lift devices deployed, based on c		
ΔC_{Lm}	increment in maximum lift coefficient due to deployment of high-lift devices, based on c, Equation (3.2)		
ΔC_{Lml}	increment in maximum lift coefficient due to deployment of leading-edge high-lift device, based on c, see Section 5		
ΔC_{Lmt}	increment in maximum lift coefficient due to deployment of trailing-edge flap, based on c, Equation (3.4)		
$\Delta C'_{Lmt}$	increment in maximum lift coefficient due to deployment of single-slotted trailing-edge flap, based on c', at datum Reynolds number $R_c = 3.5 \times 10^6$, Equation (4.9)		
$(\Delta C'_{Lmt})_0$	component of $\Delta C'_{Lmt}$ independent of flap deflection, Equation (4.6)		
$(\Delta C'_{Lmt})_1$	component of $\Delta C'_{Lmt}$ due to flap deflection, Equation (4.6)		
ΔC_{L0}	increment in lift coefficient at zero angle of attack due to deployment of high-lift devices, based on c, Equation (3.1)		
ΔC_{L0l}	increment in lift coefficient at zero angle of attack due to deployment of leading-edge high-lift device, based on c, see Item No. 94027		
ΔC_{L0t}	increment in lift coefficient at zero angle of attack due to deployment of trailing-edge flap, based on c, Equation (3.3)		
$\Delta C'_{L0t}$	increment in lift coefficient at zero angle of attack due to deployment of single-slotted trailing-edge flap, based on c', Equation (4.1)		

$\Delta C'_{L1}$	increment in lift coefficient associated with deployment of single-slotted trailing-edge flap on aerofoil with lift-curve slope of 2π, based on c', Equation (4.1) and Figure 2		
c	basic (plain) aerofoil chord (*i.e.* chord with high-lift devices undeployed), see Sketch 4.1	m	ft
c'	extended aerofoil chord (*i.e.* chord with high-lift devices deployed), see Sketch 4.1 and Equation (4.4)	m	ft
c_{t1}	chord of single-slotted trailing-edge flap, see Sketch 4.1	m	ft
c'_{t1}	extended flap chord, see Sketch 4.1 and Equation (4.5)	m	ft
Δc_l	chord extension due to deployment of leading-edge device, see Sketch 4.1	m	ft
Δc_{t1}	increment in chord of single-slotted trailing-edge flap, see Sketch 4.1	m	ft
F_R	factor for effect of Reynolds number on ΔC_{Lml} and ΔC_{Lmt}, see Equation (3.5)		
J_{t1}	correlation factor (efficiency factor) for single-slotted trailing-edge flap, Equation (4.2) or (4.3) or Figure 1		
K_l	correlation factor for effect of leading-edge device deflection, see Section 5		
K_T	correlation factor for effect of basic aerofoil geometry, Figure 3		
K_{t1}	correlation factor for effect of deflection of single-slotted trailing-edge flap, Figure 4		
M	free-stream Mach number		
R_c	Reynolds number based on free-stream conditions and aerofoil chord c		
t	maximum thickness of aerofoil	m	ft
x	chordwise distance aft from basic aerofoil leading edge	m	ft
x_{ts}	chordwise location of flap-shroud trailing edge, see Sketch 4.1	m	ft
x_{um}	chordwise location of maximum upper-surface ordinate	m	ft
$z_{u1.25}$	upper-surface ordinate at $x = 0.0125c$ for basic aerofoil	m	ft
δ_l, δ_l°	deflection of leading-edge device, see Sketch 4.1	rad, deg	rad, deg
δ_{t1}, δ_{t1}°	deflection of trailing-edge flap, positive trailing edge down, see Sketch 4.1	rad, deg	rad, deg

ρ_l	leading-edge radius of basic aerofoil, see Sketch 4.1	m	ft

Subscripts

$(\ )_{expt}$	denotes experimental value
$(\ )_{pred}$	denotes predicted value

2. INTRODUCTION

2.1 Scope of the Item

This Item provides semi-empirical methods for estimating the incremental effects on aerofoil lift at zero angle of attack and on maximum lift due to the deployment of a single-slotted trailing-edge flap, with or without the deployment of a leading-edge device, at low speeds.

Section 3 summarises the equations relating the contributions to the total lift increments at zero angle of attack and at maximum lift arising from the deployment of leading-edge high-lift devices and trailing-edge flaps. Section 4 presents methods whereby the contributions from single-slotted trailing-edge flaps are obtained. The contribution to the lift increment at zero angle of attack arising from a variety of leading-edge high-lift devices is obtainable from Item No. 94027 (Derivation 26). However, with regard to the lift increment at maximum lift, the situation is hampered by the lack of test data for other than slats in combination with slotted flaps. Nevertheless, Section 5 provides a guide to the use of the data in Item No. 94027 in the present context for the full range of leading-edge high-lift devices covered in that Item.

Section 6 concerns applicability and accuracy, Section 7 gives the Derivation and References and Section 8 presents two detailed examples illustrating the use of the methods.

2.2 Application of Data to Calculation of Total Lift Coefficient Values C_{L0} and C_{Lm}

In order to use the data obtained from the present Item in the wider context in which the total lift coefficient at zero angle of attack, C_{L0}, and at maximum lift, C_{Lm}, are required for an aerofoil with high-lift devices deployed, it is necessary to refer to Item No. 94026 (Reference 29). That Item acts as an introduction to, and a link between, each of the Items in the complete series dealing with the incremental effects of high-lift device deployment on aerofoil lift at zero angle of attack and on maximum lift. It describes how the incremental effects are summed and added to the contributions from the basic (*i.e.* plain) aerofoil to give the total values C_{L0} and C_{Lm}.

3. LIFT COEFFICIENT INCREMENTS ΔC_{L0} AND ΔC_{Lm}

The increments in the lift coefficient at zero angle of attack, ΔC_{L0}, and at maximum lift, ΔC_{Lm}, due to the deployment of a leading-edge high-lift device and a trailing-edge flap on an aerofoil are given by the sum of the individual increments, *i.e.*

$$\Delta C_{L0} = \Delta C_{L0l} + \Delta C_{L0t} \tag{3.1}$$

and

$$\Delta C_{Lm} = \Delta C_{Lml} + \Delta C_{Lmt}. \tag{3.2}$$

The increments in Equations (3.1) and (3.2) are based on the chord, c, of the basic aerofoil.

The values of ΔC_{L0l} and ΔC_{Lml} for various leading-edge devices are obtainable from Item No. 94027. However, see Section 5 with regard to ΔC_{Lml} for use with the present Item.

For correlation purposes it is more convenient to present the right-hand sides of Equations (3.1) and (3.2) in terms of increments based on the extended chord c'. Also, whereas values of ΔC_{L0l} and ΔC_{L0t} can be taken to be independent of Reynolds number, the values of ΔC_{Lml} and ΔC_{Lmt} are influenced by Reynolds number. Thus, for a general trailing-edge flap, Item No. 94028 (Derivation 27) shows that

$$\Delta C_{L0t} = \frac{c'}{c}\Delta C'_{L0t} \tag{3.3}$$

and

$$\Delta C_{Lmt} = F_R \frac{c'}{c}\Delta C'_{Lmt} \tag{3.4}$$

where

$$F_R = 0.153\log_{10} R_c\,. \tag{3.5}$$

The value of $\Delta C'_{Lmt}$ in Equation (3.4) is therefore appropriate to the datum Reynolds number $R_c = 3.5 \times 10^6$, for which $F_R = 1$, (see Section 6.1).

The values of $\Delta C'_{L0t}$ and $\Delta C'_{Lmt}$ in Equations (3.3) and (3.4) are determined for single-slotted trailing-edge flaps by the methods of Section 4.

4. LIFT COEFFICIENT INCREMENTS $\Delta C'_{L0t}$ AND $\Delta C'_{Lmt}$

First approximations to the lift coefficient increments due to the deployment of trailing-edge flaps can be obtained from the theory for an equivalent thin hinged plate with empirical correlation factors to account for the geometry of practical aerofoils and flaps. To make some allowance for the effects of chord extension in the theory, the flap-chord ratio and the lift coefficient increments are based on the aerofoil extended chord. This approach was used in Derivation 22 and was the basis for the methods developed for plain trailing-edge flaps in Item No. 94028 which was used as a model for the methods given in the present Item for single-slotted trailing-edge flaps, see Sections 4.1 and 4.2. However, some adjustments were required to adapt to the considerable departure from the thin hinged plate basis of the model when applied to a slotted flap, possibly involving large extensions in chord.

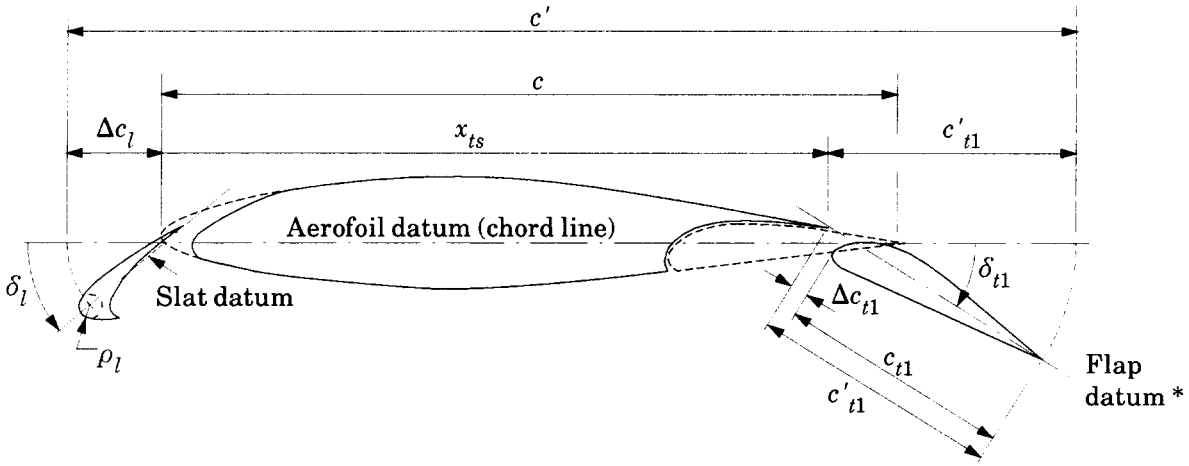

* Flap datum is rotated aerofoil datum

Sketch 4.1 Single-slotted trailing-edge flap with typical leading-edge high-lift device (slat)

4.1 Increment in Lift Coefficient at Zero Angle of Attack

The increment in lift coefficient at zero angle of attack due to the deployment of a single-slotted trailing-edge flap is given by

$$\boxed{\Delta C'_{L0t} = J_{t1}\Delta C'_{L1}\,(a_1)_0/2\pi\,.} \tag{4.1}$$

In this equation J_{t1} is an empirical correlation (or efficiency) factor which is a function of δ_{t1} and is given by

$$J_{t1} = 1.17[\sin(3.83\delta^\circ_{t1})]^{\frac{1}{2}} \qquad \text{for } 0 \le \delta^\circ_{t1} \le 23.5^\circ \tag{4.2}$$

and

$$J_{t1} = 1.17 \qquad \text{for } \delta^\circ_{t1} > 23.5^\circ\,, \tag{4.3}$$

which are plotted in Figure 1.

The flap deflection, δ_{t1}, is seen from Sketch 4.1 to be the angle through which the flap datum* is rotated relative to the stowed flap situation. Thus, for a single-slotted flap δ_{t1} is the angle through which the aerofoil datum is rotated.

The lift coefficient increment, $\Delta C'_{L1}$, associated with the deployment of a single-slotted flap on an aerofoil having a lift-curve slope of 2π, is based on Item No. Flaps 01.01.08 (Derivation 19) and is given in Figure 2 as a function of δ°_{t1} and c'_{t1}/c'. The parameter $\Delta C'_{L1}$, which is based on test data, replaces the value derived from thin plate theory used for plain flaps in Item No. 94028. This was necessary because slot effects are not represented in the simple theory.

The aerofoil extended chord, c', in Sketch 4.1 is given by

$$c' = \Delta c_l + x_{ts} + c'_{t1}\,. \tag{4.4}$$

The parameter Δc_l is the chord extension due to the deployment of the leading-edge device, obtained for a variety of such devices from Item No. 94027. The quantity x_{ts} is the chordwise location of the trailing-edge of the flap shroud and the extended chord length of the flap, c'_{t1}, is given by

$$c'_{t1} = c_{t1} + \Delta c_{t1}\,. \tag{4.5}$$

In Sketch 4.1 Δc_{t1} is drawn as having a magnitude sufficiently small to neglect. For those cases in which Δc_{t1} is not small, graphical estimation would be necessary.

The parameter $(a_l)_0$ in Equation (4.1) is the basic aerofoil lift-curve slope in incompressible flow from Item No. Wings 01.01.05 (Derivation 21).

The value of $\Delta C'_{L0t}$ is then used in Equation (3.3) to determine ΔC_{L0t}.

4.2 Increment in Maximum Lift Coefficient

In the development of the method for predicting the increment in maximum lift coefficient it was found necessary to adapt further the thin hinged plate theoretical model to cater for slotted flaps, especially those involving large chord extensions, *i.e.* Fowler flaps. With such flaps it is possible to obtain significant

* Note that for a single-slotted flap the flap datum is taken as the rotated aerofoil datum, not the flap chord.

increments in maximum lift (with a low drag penalty) by deployment with zero deflection. The increment in maximum lift is then very largely due to chord extension and is related to the basic aerofoil maximum lift. The increment in maximum lift coefficient then consists of two components, one, $(\Delta C'_{Lmt})_0$, independent of flap deflection and the other, $(\Delta C'_{Lmt})_1$, due to the deflection. Thus

$$\Delta C'_{Lmt} = (\Delta C'_{Lmt})_0 + (\Delta C'_{Lmt})_1, \tag{4.6}$$

where

$$(\Delta C'_{Lmt})_0 = (1 - c/c')(C_{LmB})_d \tag{4.7}$$

and

$$(\Delta C'_{Lmt})_1 = K_T K_{t1} J_{t1} \Delta C'_{L1} - (1 - c/c')\sin\delta_{t1}(C_{LmB})_d, \tag{4.8}$$

so that

$$\boxed{\Delta C'_{Lmt} = (1 - c/c')(1 - \sin\delta_{t1})(C_{LmB})_d + K_T K_{t1} J_{t1} \Delta C'_{L1}\,.} \tag{4.9}$$

In Equation (4.9) $(C_{LmB})_d$ is the maximum lift coefficient for the basic aerofoil at the datum Reynolds number $R_c = 3.5 \times 10^6$, obtained from Item No. 84026 (Derivation 25).

The extended chord, c', is given by Equations (4.4) and (4.5), J_{t1} is obtained either from Figure 1 or from Equation (4.2) or (4.3) and $\Delta C'_{L1}$ is obtained from Figure 2.

The correlation factor K_T, given in Figure 3, allows for the effect of basic aerofoil geometry via $z_{u1.25}/c$, the dimensionless upper-surface ordinate at $0.0125c$, and x_{um}/c, the dimensionless chordwise location of the maximum upper-surface ordinate. Values of $z_{u1.25}/c$ for a range of NACA sections are given in Item No. 66034 (Reference 28). The correlation factor K_{t1} is given as a function of δ°_{t1} in Figure 4.

Finally, with the value of $\Delta C'_{Lmt}$ obtained from Equation (4.9), ΔC_{Lmt} is evaluated from Equation (3.4) with F_R given by Equation (3.5).

5. EFFECT OF LEADING-EDGE HIGH-LIFT DEVICE

The only leading-edge device for which test data are available for aerofoils with slotted trailing-edge flaps is the slat. With regard to the effect of slat deployment on the lift coefficient at zero angle of attack it was found that the increment determined from Item No. 94027 could be used without modification. That being so, it is anticipated that for ΔC_{L0l} the methods of Item No. 94027 for any leading-edge device may be used in conjunction with the present Item for single-slotted flaps.

Unfortunately, the analysis with regard to maximum lift revealed a more complicated picture. It was found that the optimum slat gap with slotted flaps deployed is larger than for the situation in which the flap is undeployed. The optimum gap is typically within the range $0.02c$ to $0.05c$ with slotted flaps deployed, compared with about $0.01c$ for the flaps undeployed case, for the same range of slat angles. However, only a small variation in ΔC_{Lm} was found within that range, and the test data were used to derive a modified variation of the slat correlation factor K_l with δ°_l compared to those given in Figure 1b of Item No. 94027. The revised factor, which applies only to an optimum (or near-optimum) design, is given in Figure 5. Apart

from the value of K_l the method of Item No. 94027 for slats can be assumed to be unchanged.

Since Figure 1b in Item No. 94027 applies to both slats and vented Krüger flaps it is anticipated that Figure 5 in the present Item will likewise be applicable to optimised vented Krüger flaps. Further, since the slot flow for the leading-edge device is deemed to be responsible for the changes in K_l, it is felt reasonable to assume that for leading-edge devices with no slot the methods of Item No. 94027 can be used unchanged. However, in the absence of appropriate test data the use of Item No. 94027 for leading-edge devices other than slats in conjunction with the present Item for single-slotted flaps should be treated with caution in terms of maximum lift.

Finally, it is important to remember that if the leading-edge device extends the aerofoil chord when deployed (*i.e.* $\Delta c_l > 0$, see Equation (4.4)) the effect of that chord extension on c' needs to be taken into account when evaluating Equations (4.1) and (4.9) for the trailing-edge flap.

6. APPLICABILITY AND ACCURACY

6.1 Applicability

Methods are given in this Item for estimating the increments in aerofoil lift coefficient at zero angle of attack and in maximum lift coefficient due to the deployment of a single-slotted trailing-edge flap with or without the deployment of a leading-edge high-lift device.

Table 6.1 summarises the parameter ranges covered by the measured data, obtained from Derivations 1 to 18, 20, 23 and 24, from which the various correlation parameters have been obtained. Although test data (Derivations 23 and 24) were available for single-slotted trailing-edge flaps in conjunction with only one type of leading-edge high-lift device (slat) it is anticipated that, with caution, the methods will apply to any of the types of leading-edge device treated in Item No. 94027, (but see Section 5).

The methods in Section 4 were derived using measured data from wind-tunnel models for which attempts had been made to determine optimum values of the laps and gaps for the slots. The correlations (see Section 6.2) include many data points for which the lap and gap values were near to but not at the optimum, from investigations to find the optimum at each flap deflection. The methods, particularly that for the increment in maximum lift coefficient, therefore apply only to configurations in which the laps and gaps are close to the optimum.

The value $R_c = 3.5 \times 10^6$ was used as the datum from which to develop the factor F_R applicable to the increment in maximum lift coefficient, see Section 3. Most of the data were at or around this value. The effect of Reynolds number on ΔC_{L0t} over the parameter ranges given in Table 6.1 and for higher Reynolds numbers can be assumed to be negligible.

TABLE 6.1 Parameter ranges for test data for single-slotted trailing-edge flaps used in methods of Section 4

Parameter	*Ranges*
t/c	0.10 to 0.30
ρ_l/c	0.007 to 0.099
$z_{u1.25}/c$	0.013 to 0.072
x_{um}/c	0.25 to 0.45
x_{ts}/c	0.715 to 1.000
c_{t1}/c	0.15 to 0.40
δ°_{t1}	0 to 60°
c'/c (no slat)	1.02 to 1.42
c'/c (with slat)	1.27 to 1.39
$R_c \times 10^{-6}$	1.0 to 9.0
M	0.12 to 0.24

The method of the Item takes no account of Mach number in the increments in maximum lift coefficient due to the deployment of high-lift devices. This is not because such effects are felt to be insignificant, since even at quite low free-stream Mach numbers the local flow around a leading-edge device can attain supersonic velocities. Rather, it is due to the lack of data for free-stream Mach numbers greater than 0.24 for the type of high-lift device considered. It is however suggested that the use of the Item be restricted to $M \leq 0.2$ for consistency with the other Items in the series.

6.2 Accuracy

Sketch 6.1 shows the comparison between predicted and experimental values of ΔC_{L0} due to the deployment of single-slotted trailing-edge flaps. Also shown are comparisons for single-slotted flaps in combination with leading-edge slats. With few exceptions the predicted and test data for ΔC_{L0} are correlated to within $\pm 15\%$.

Similarly Sketch 6.2 presents the corresponding values of the increment in maximum lift coefficient. With few exceptions the data for ΔC_{Lm} are correlated to within $\pm 15\%$.

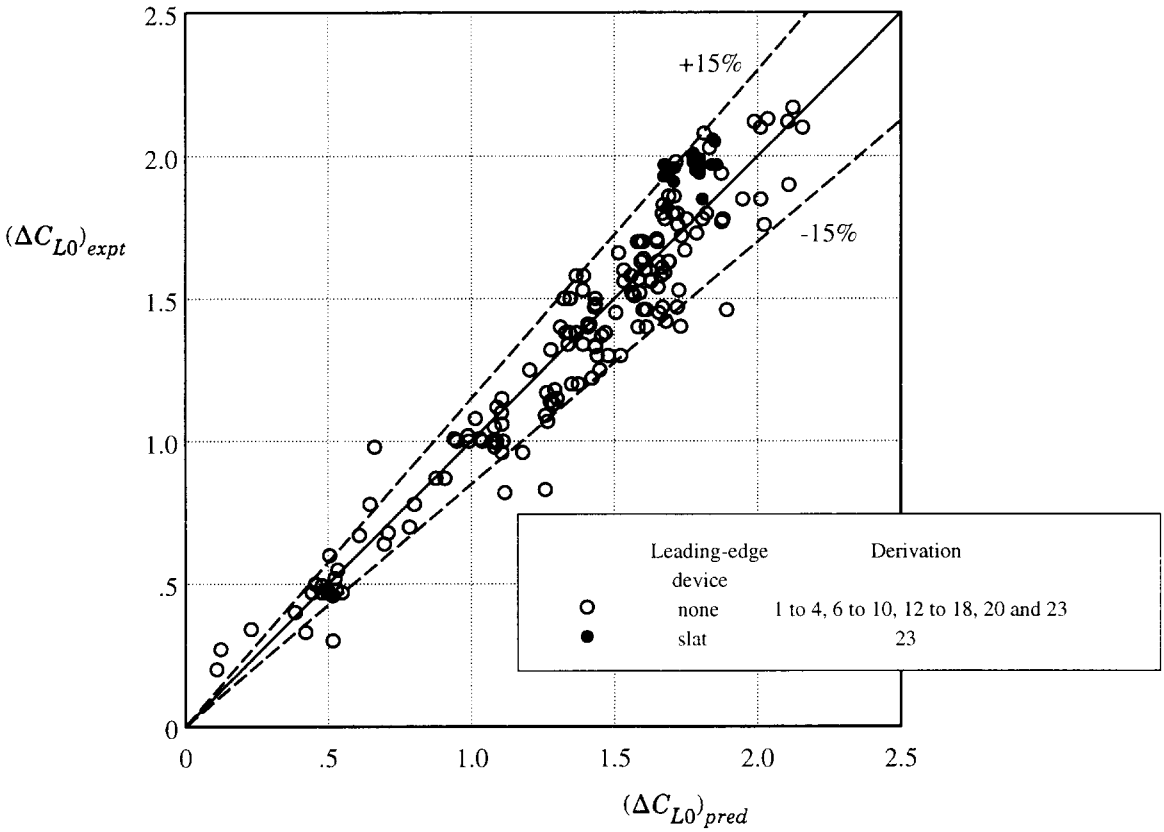

Sketch 6.1 Comparison of predicted and experimental values of ΔC_{L0}

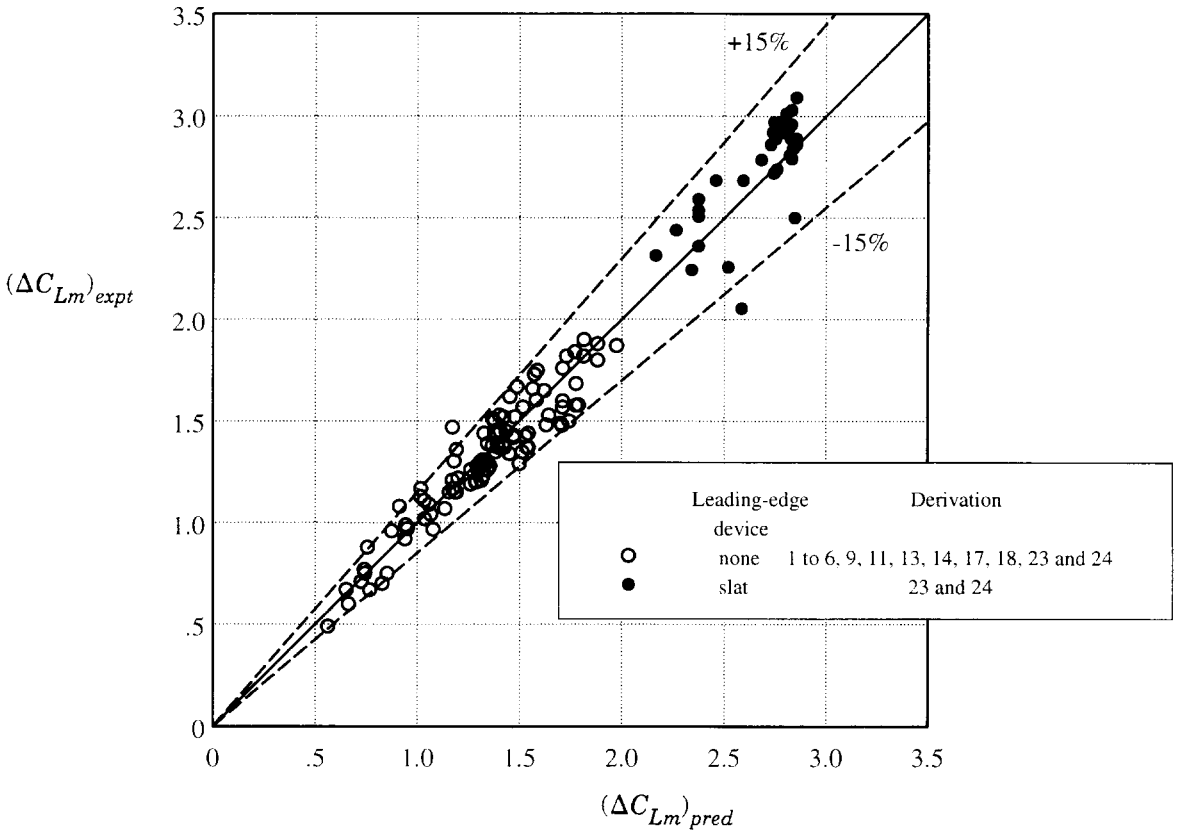

Sketch 6.2 Comparison of predicted and experimental values of ΔC_{Lm}

7. DERIVATION AND REFERENCES

7.1 Derivation

The Derivation lists selected sources of information that have assisted in the preparation of this Item.

1. PLATT, R.C. — Aerodynamic characteristics of a wing with Fowler flaps including flap loads, downwash and calculated effect on take-off. NACA Rep. 534, 1935.

2. WENZINGER, C.J. HARRIS, T.A. — Wind-tunnel investigation of an NACA 23012 airfoil with various arrangements of slotted flap. NACA Rep. 664, 1938.

3. WENZINGER, C.J. GAUVAIN, W.E. — Wind-tunnel investigation of an NACA 23012 airfoil with a slotted flap and three types of auxiliary flap. NACA Rep. 679, 1938.

4. WENZINGER, C.J. HARRIS, T.A. — Wind-tunnel investigation of an NACA 23021 airfoil with various arrangements of slotted flaps. NACA tech. Note 677, 1939.

5. DUSCHIK, F. — Wind-tunnel investigation of an NACA 23021 airfoil with two arrangements of a 40 per cent chord slotted flap. NACA tech. Note 728, 1939.

6. RECANT, I.G. — Wind-tunnel investigation of an NACA 23030 airfoil with various arrangements of slotted flaps. NACA tech. Note 755, 1940.

7. HARRIS, T.A. PURSER, P.E. — Wind-tunnel investigation of an NACA 23012 airfoil with two sizes of balanced split flap. NACA WR L-441, 1940.

8. SWANSON, R.S. SCHULDENFREI, M.J. — Wind-tunnel investigation of an NACA 23021 airfoil with two sizes of balanced split flaps. NACA WR L-449 (ARC 5576), 1941.

9. LOWRY, J.G. — Wind-tunnel investigation of an NACA 23012 airfoil with several arrangements of slotted flaps with extended lips. NACA tech. Note 808, 1941.

10. UNDERWOOD, W.J. ABBOTT, F.T. — Test of NACA 66, 2-116, a = 0.6 airfoil section fitted with pressure balance and slotted flaps for the wing of the XP 63 airplane. NACA WR L-701, 1942.

11. ABBOTT, I.H. — Tests of four models representing intermediate sections of the XB 33 airplane, including sections with slotted flap and ailerons. NACA WR L-704 (TIL 1578), 1942.

12. BOGDONOFF, S.M. — Test of two models representing intermediate inboard and outboard wing sections of the XB 36 airplane. NACA WR L-662 (TIL 1581), 1943.

13. HOLTZCLAW, R.W. WEISMAN, Y. — Wind-tunnel investigation of the effects of slot shape and flap location on the characteristics of a low drag airfoil equipped with a 0.25-chord slotted flap. NACA WR A-80 (TIL 1494), 1944.

14. HOLTZCLAW, R.W. — Wind-tunnel investigation of the effects of spoilers on the characteristics of a low drag airfoil equipped with a 0.25-chord slotted flap. NACA MR A5G23 (TIL 1625), 1945.

15. LOFTIN, L.K. RICE, F.J. — Two-dimensional wind-tunnel investigation of two NACA low drag airfoil sections equipped with slotted flaps. NACA WR L5L11 (TIL 1453), 1946.

16. CAHILL, J.F. — Two-dimensional wind-tunnel investigation of four types of high lift flap on a NACA 65-210 airfoil section. NACA tech. Note 1191, 1947.

17. RACISZ, S.F. — Investigation of NACA 65(112)A111 (approx.) airfoil with 0.35-chord slotted flap at Reynolds numbers up to 25 million. NACA tech. Note 1463, 1947.

18. CAHILL, J.F. — Summary of section data on trailing-edge high-lift devices. NACA Rep. 938, 1949.

19. ESDU — Lift coefficient increment due to full-span slotted flaps. ESDU International, Item No. Flaps 01.01.08, 1949.

20. GOODWIN, M.D. — Single-slotted trailing-edge flap combined with plain or slotted leading-edge flap. WADC TR 6356, Part 3, 1953.

21. ESDU — Slope of lift curve for two-dimensional flow. ESDU International, Item No. Wings 01.01.05, 1955.

22. SCHEMENSKY, R.T. — Development of an empirically based computer program to predict the aerodynamic characteristics of aircraft. Volume 1: Empirical methods. Convair Aerospace Division, General Dynamics Corporation. AFFDL TR-73-144 (AD 780 100), 1973.

23. LJUNGSTROM, B.L.G. — Two-dimensional wind-tunnel experiments with single and double slotted flaps. Aeronaut. Res. Inst., Sweden. FFA AU-1083, 1975.

24. BAe, Weybridge — Unpublished wind-tunnel test data, 1970 to 1980.

25. ESDU — Aerofoil maximum lift coefficient for Mach numbers up to 0.4. ESDU International, Item No. 84026, 1984.

26. ESDU — Increments in aerofoil lift coefficient at zero angle of attack and in maximum lift coefficient due to deployment of various leading-edge high-lift devices at low speeds. ESDU International, Item No. 94027, 1994.

27. ESDU — Increments in aerofoil lift coefficient at zero angle of attack and in maximum lift coefficient due to deployment of a plain trailing-edge flap, with or without a leading-edge high-lift, device at low speeds. ESDU International, Item No. 94028, 1994.

7.2 References

The References list selected sources of information supplementary to that given in this Item.

28. ESDU — The low-speed stalling characteristics of aerodynamically smooth aerofoils. ESDU International, Item No. 66034, 1966.

29. ESDU — Introduction to the estimation of the lift coefficients at zero angle of attack and at maximum lift for aerofoils with high-lift devices at low speeds. ESDU International, Item No. 94026, 1994.

8. EXAMPLES

8.1 Example 1: Single-slotted Flap

The incremental effects on the lift coefficient at zero angle of attack and on the maximum lift coefficient are to be estimated for a single-slotted flap deployed at 30° on a modified smooth NACA 65_2-215 aerofoil as shown in Sketch 8.1. The modifications produced a linear profile rearwards from 75% chord and 65% chord on the upper and lower surfaces respectively.

The relevant geometrical data are

Aerofoil			Flap		
t/c	=	0.15	c_{t1}	=	0.8 ft
c	=	2.5 ft	δ°_{t1}	=	30°
$z_{u1.25}/c$	=	0.0188	Δc_{t1}	=	0
x_{um}/c	=	0.40	x_{ts}	=	2.25 ft

The flow conditions are

$M = 0.2$ and $R_c = 3.5 \times 10^6$.

Also given for the modified NACA 65_2-215 are

$(a_1)_0 = 5.62$ rad^{-1} from Item No. W.01.01.05 for boundary-layer transition at the leading edge

and $(C_{LmB})_d = 1.309$ from Item No. 84026 for a smooth aerofoil surface at $R_c = 3.5 \times 10^6$.

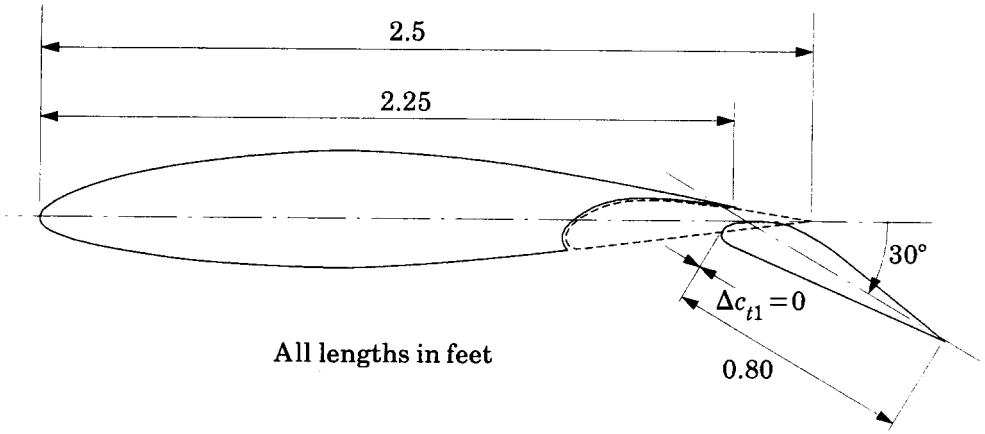

Sketch 8.1

The extended flap chord c'_{t1} , shown in Sketch 4.1, is given by Equation (4.5) as

$$\begin{aligned} c'_{t1} &= c_{t1} + \Delta c_{t1} \\ &= 0.8 + 0 \\ &= 0.8 \text{ ft.} \end{aligned}$$

The aerofoil extended chord c' is given by Equation (4.4) as

$$c' = \Delta c_l + x_{ts} + c'_{t1}$$

and since there is no leading-edge device $\Delta c_l = 0$, so that

$$\begin{aligned} c' &= 0 + 2.25 + 0.8 \\ &= 3.05 \text{ ft.} \end{aligned}$$

Therefore,

$$\begin{aligned} c'_{t1}/c' &= 0.8/3.05 \\ &= 0.262 \end{aligned}$$

and

$$\begin{aligned} c'/c &= 3.05/2.5 \\ &= 1.22. \end{aligned}$$

Calculation of ΔC_{L0t}:

From Equation (4.1)

$$\Delta C'_{L0t} = J_{t1} \Delta C'_{L1} (a_1)_0/2\pi.$$

From Equation (4.3)

$$J_{t1} = 1.17 \text{ for } \delta^\circ_{t1} = 30^\circ.$$

From Figure 2 with $\delta^\circ_{t1} = 30^\circ$ and $c'_{t1}/c' = 0.262$

$$\Delta C'_{L1} = 1.26.$$

Hence

$$\begin{aligned} \Delta C'_{L0t} &= 1.17 \times 1.26 \times 5.62/2\pi \\ &= 1.319, \end{aligned}$$

so that from Equation (3.3)

$$\begin{aligned}\Delta C_{L0t} &= (c'/c)\Delta C'_{L0t}\\ &= 1.22 \times 1.319\\ &= 1.61.\end{aligned}$$

Calculation of ΔC_{Lmt}:

From Figure 3 with $z_{u1.25}/c = 0.0188$ and $x_{um}/c = 0.4$

$$K_T = 2.5$$

and from Figure 4 with $\delta°_{t1} = 30°$

$$K_{t1} = 0.35.$$

Equation (4.9) gives

$$\begin{aligned}\Delta C'_{Lmt} &= (1 - c/c')(1 - \sin\delta_{t1})(C_{LmB})_d + K_T K_{t1} J_{t1} \Delta C'_{L1}\\ &= (1 - 1/1.22) \times (1 - \sin 30°) \times 1.309 + 2.5 \times 0.35 \times 1.17 \times 1.26\\ &= 0.118 + 1.290\\ &= 1.408.\end{aligned}$$

Equation (3.5) gives, for $R_c = 3.5 \times 10^6$,

$$\begin{aligned}F_R &= 0.153 \log_{10} R_c\\ &= 0.153 \times \log_{10}(3.5 \times 10^6)\\ &= 1.00.\end{aligned}$$

Therefore, Equation (3.4) gives

$$\begin{aligned}\Delta C_{Lmt} &= (c'/c)\Delta C'_{Lmt}\\ &= 1.00 \times 1.22 \times 1.408\\ &= 1.72.\end{aligned}$$

8.2 Example 2: Single-slotted Flap with Leading-edge Slat

Estimate the effects on the lift coefficient at zero angle of attack and on the maximum lift coefficient of the addition of an optimised leading-edge slat to the single-slotted flap configuration considered in Example 1, as shown in Sketch 8.2. The relevant geometrical data for the slat (using the notation of Item No. 94027) are

$$c_l = 0.46 \text{ ft} \qquad \rho_l/c = 0.01505$$
$$\delta_l^\circ = 40^\circ (\delta_l = 0.698 \text{ rad}) \qquad H_l = 0.04 \text{ ft}$$
$$x_n = 0.10 \text{ ft} \qquad G_l = 0.05 \text{ ft}$$
$$x_l = 0.43 \text{ ft} \qquad L_l = -0.02 \text{ ft}$$

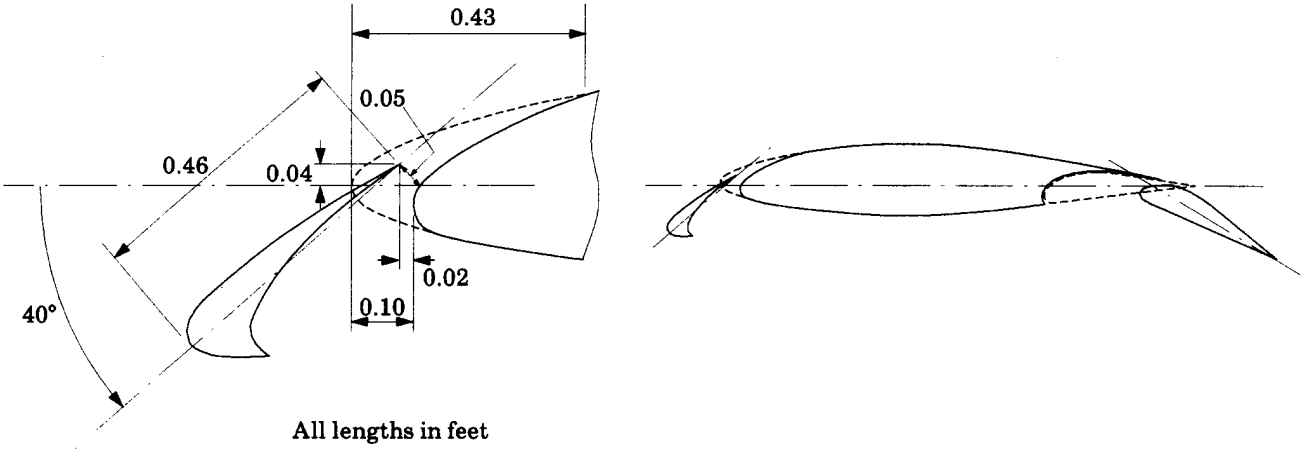

Sketch 8.2

As noted in Section 5 the effect of the deployed slat is to increase the extended chord c', with the result that the calculations for ΔC_{L0t} and ΔC_{Lmt} from Example 1 will need to be revised for the changed values of c'_{t1}/c' and c'/c.

From Item No. 94027 Equation (4.4a), the chord extension due to slat deployment is

$$\begin{aligned} \Delta c_l &= c_l - x_n - L_l - H_l \tan(\delta_l^\circ/2) \\ &= 0.46 - 0.10 - (-0.02) - 0.04 \times \tan(40^\circ/2) \\ &= 0.365 \text{ ft.} \end{aligned}$$

The extended chord c' is obtained from Equation (4.4), with values of c'_{t1} and x_{ts} from Example 1, as

$$\begin{aligned} c' &= \Delta c_l + x_{ts} + c'_{t1} \\ &= 0.365 + 2.25 + 0.8 \\ &= 3.415 \text{ ft} \end{aligned}$$

and so

$$\begin{aligned} c'/c &= 3.415/2.5 \\ &= 1.366. \end{aligned}$$

Therefore, for the slat (in the notation of Item No. 94027)

$$c_{el}/c' = c_l/c' = 0.46/3.415 = 0.135,$$

and for the flap

$$c'_{t1}/c' = 0.8/3.415 = 0.234.$$

1. Slat Contributions

For the given slat geometry Item No. 94027 gives (in the notation of that Item)

$$K_0 = 1.35,\ K_e = 1,\ K_g = 1.96\ \ \delta_0 = 0.25 \text{ and } [\Delta C'_{L0l}]_2 = 0.03.$$

Figure 5* of the present Item, with $\delta°_l = 40°$, gives

$$K_l = 0.625,$$

which replaces the value that would be given by Figure 1b of Item No. 94027.

These values, together with $c_{el}/c' = 0.135$ and $\delta_l = 0.698$ rad, are then used to evaluate Equations (3.6) and (3.10) of Item No. 94027 to give

$$\Delta C'_{L0l} = -0.100 \text{ and } \Delta C'_{Lml} = 0.750,$$

respectively, which by means of Equations (3.7) and (3.12) of Item No. 94027 with $c'/c = 1.366$ and $F_R = 1$, give

$$\Delta C_{L0l} = -0.137 \text{ and } \Delta C_{Lml} = 1.025.$$

2. Slotted-Flap Contributions

(i) *Contribution to* ΔC_{L0}:

From Figure 2 with $\delta°_{t1} = 30°$ and $c'_{t1}/c' = 0.234$

$$\Delta C'_{L1} = 1.193.$$

* Note that the value of the dimensionless slat gap $G_l/c = 0.05/2.5 = 0.02$ is within the range of applicability for Figure 5.

Hence, Equation (4.1) gives, with $J_{t1} = 1.17$ and $(a_1)_0 = 5.62$ rad^{-1} from Example 1,

$$\begin{aligned}\Delta C'_{L0t} &= J_{t1}\Delta C'_{L1}\,(a_1)_0/2\pi \\ &= 1.17 \times 1.193 \times 5.62/2\pi \\ &= 1.248,\end{aligned}$$

so that, from Equation (3.3)

$$\begin{aligned}\Delta C_{L0t} &= (c'/c)\Delta C'_{L0t} \\ &= 1.366 \times 1.248 \\ &= 1.705.\end{aligned}$$

(ii) *Contribution to* ΔC_{Lm}:

Equation (4.9) gives, for $c'/c = 1.366$, $\Delta C'_{L1} = 1.193$ and the remaining parameter values from Example 1,

$$\begin{aligned}\Delta C'_{Lmt} &= (1 - c/c')(1 - \sin\delta_{t1})(C_{LmB})_d + K_T K_{t1} J_{t1}\Delta C'_{L1} \\ &= (1 - 1/1.366) \times (1 - \sin 30°) \times 1.309 + 2.5 \times 0.35 \times 1.17 \times 1.193 \\ &= 0.176 + 1.221 \\ &= 1.397.\end{aligned}$$

Equation (3.4) then gives, with $F_R = 1$ from Example 1,

$$\begin{aligned}\Delta C_{Lmt} &= F_R(c'/c)\Delta C'_{Lmt} \\ &= 1 \times 1.366 \times 1.397 \\ &= 1.908.\end{aligned}$$

3. Total Values

Equations (3.1) and (3.2) give the total increments as

$$\begin{aligned}\Delta C_{L0} &= \Delta C_{L0l} + \Delta C_{L0t} \\ &= -0.137 + 1.705 \\ &= 1.57,\end{aligned}$$

which compares with 1.61 from Example 1 with no slat deployment, a small decrease of about 2½%, and

$$\begin{aligned}\Delta C_{Lm} &= \Delta C_{Lml} + \Delta C_{Lmt} \\ &= 1.025 + 1.908 \\ &= 2.93,\end{aligned}$$

which compares with 1.72 from Example 1 with no slat deployment, an increase of about 70%.

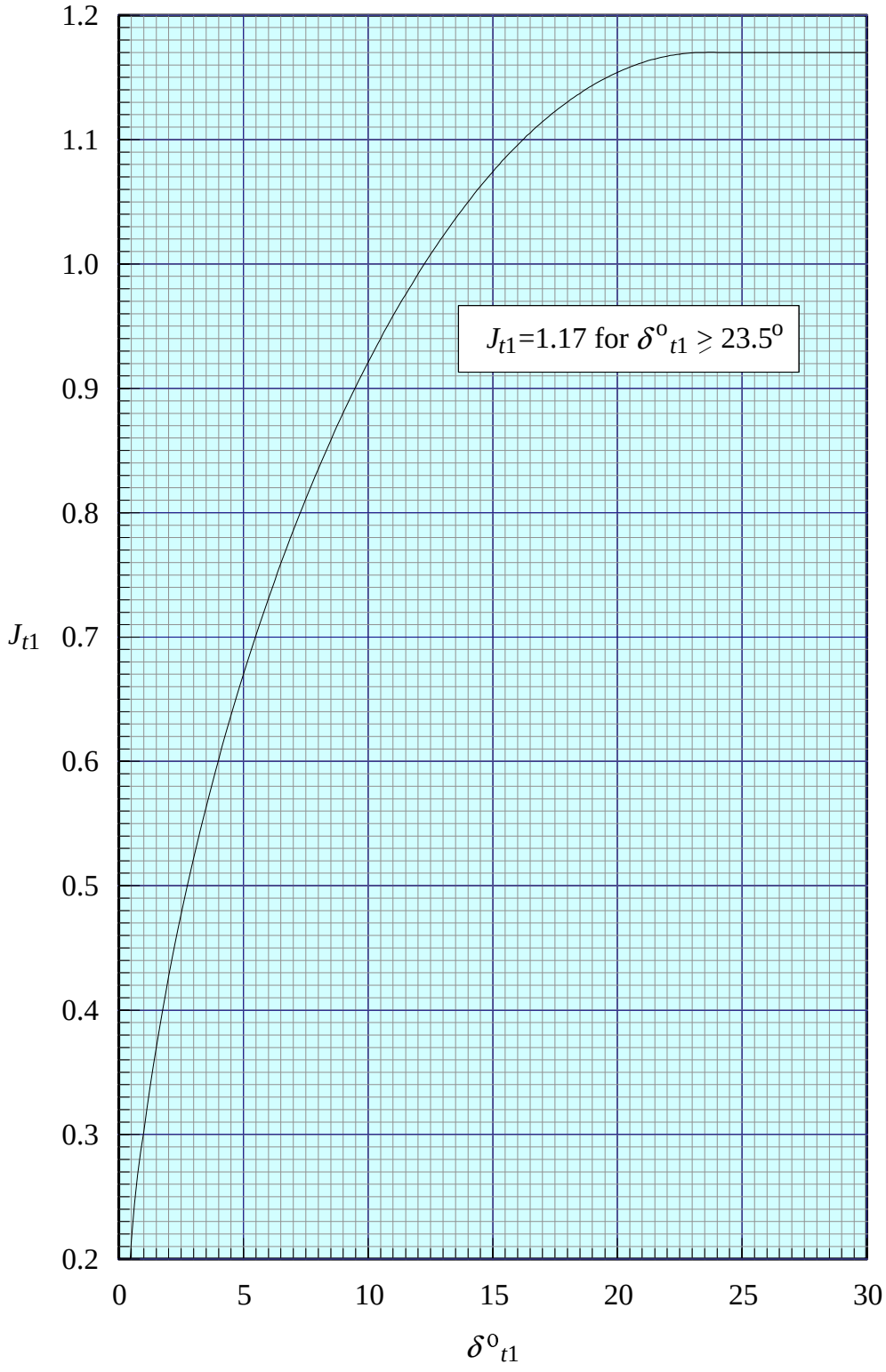
1.2
1.1
1.0
0.9
0.8
0.7
0.6
0.5
0.4
0.3
0.2
J_{t1}
J_{t1}=1.17 for $\delta^{o}_{t1} \geq 23.5^{o}$
0
5
10
15
20
25
30
δ^{o}_{t1}

FIGURE 1

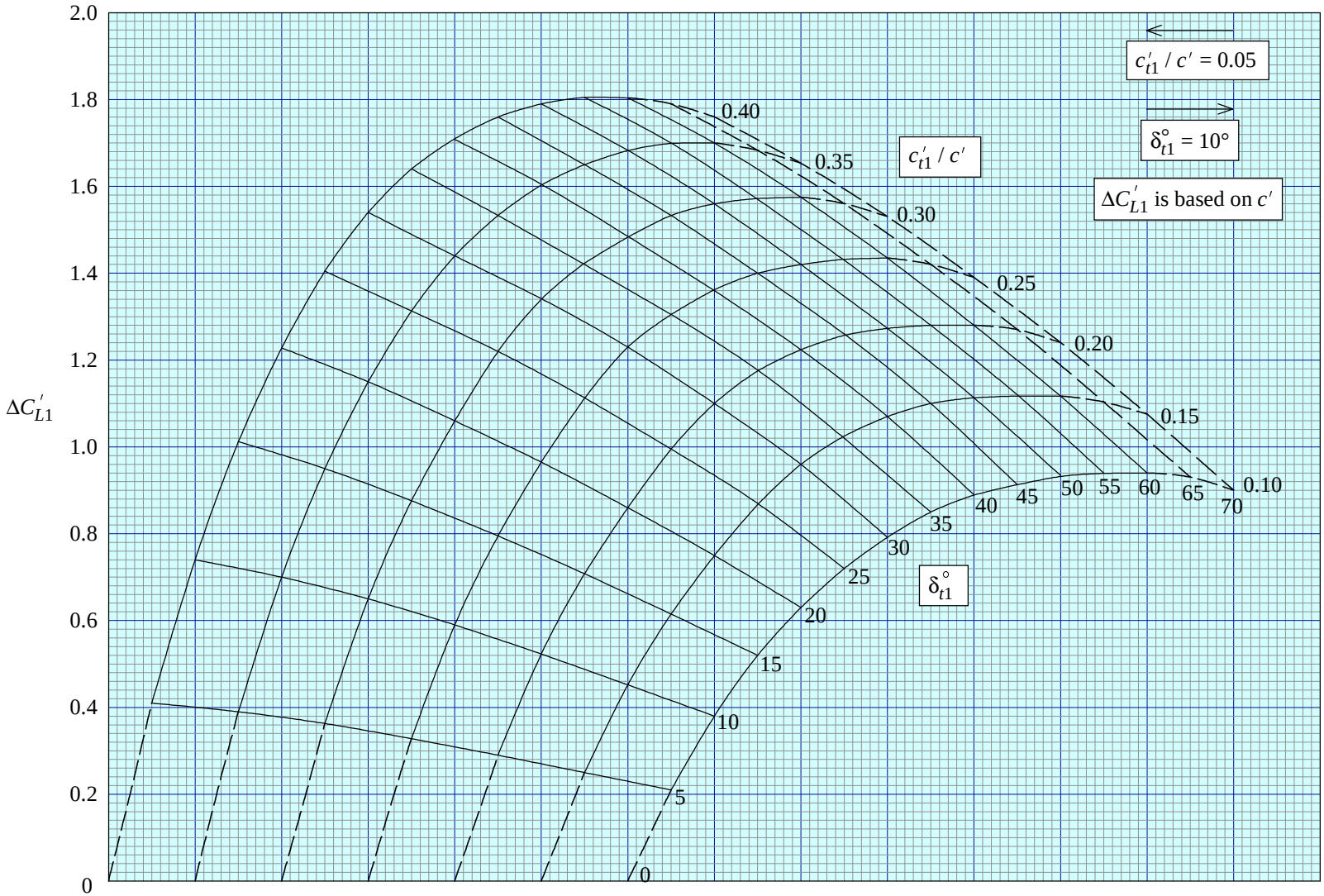

FIGURE 2

94030

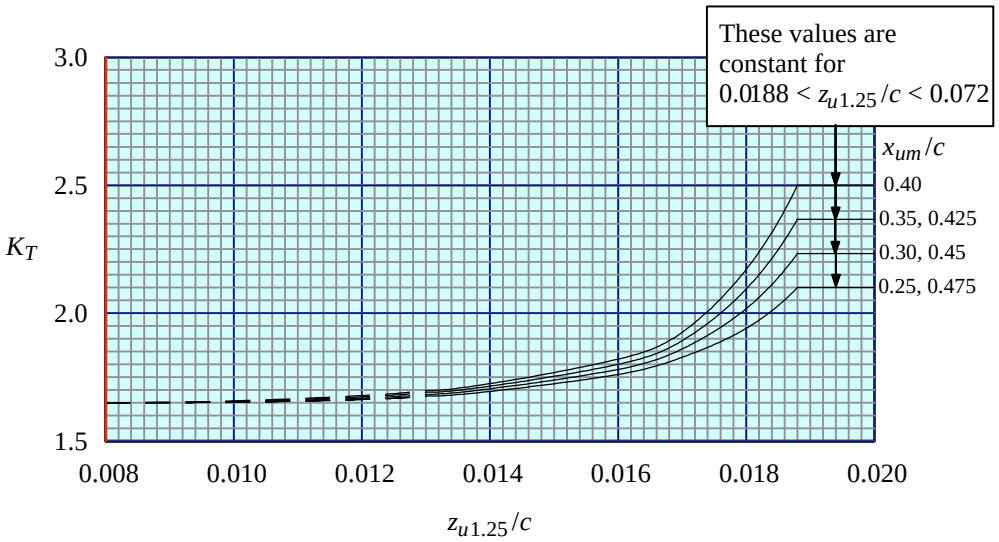

FIGURE 3

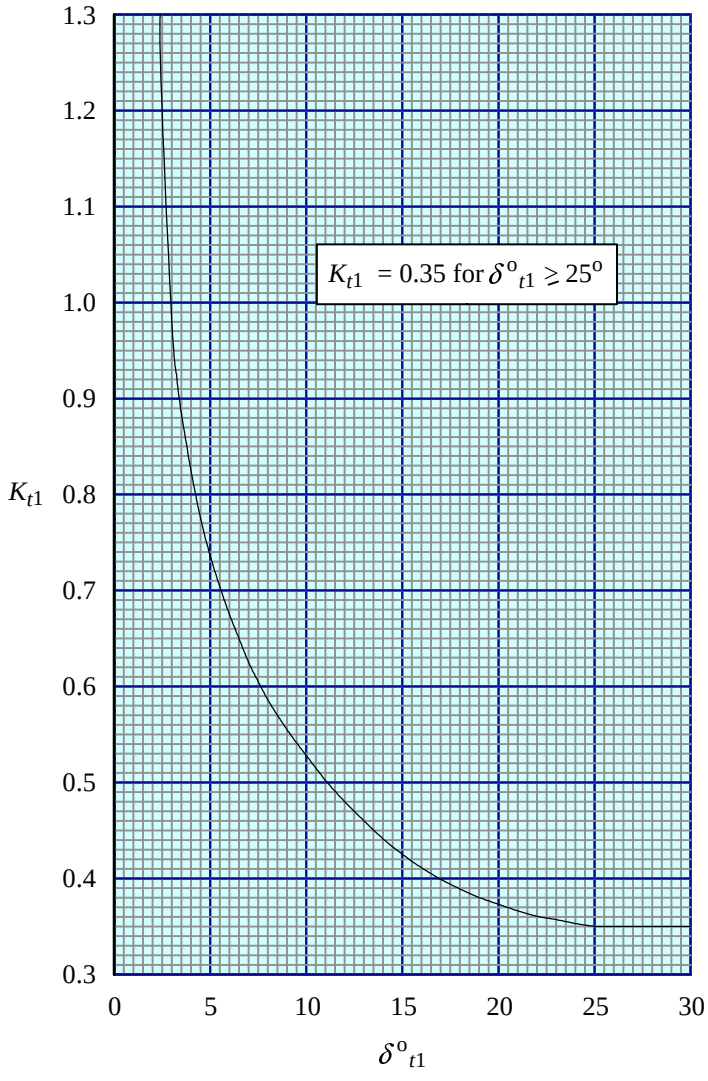

FIGURE 4

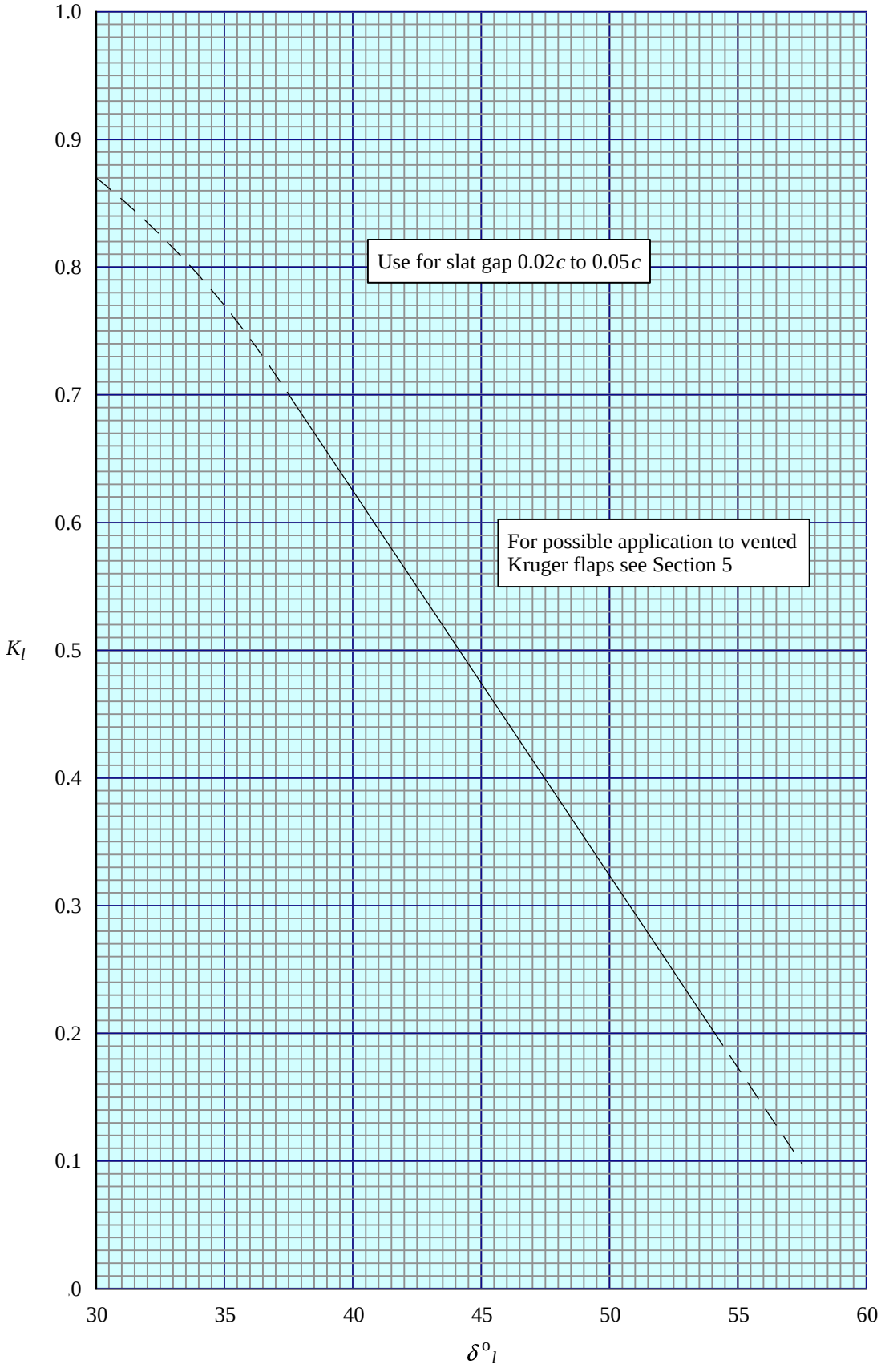

FIGURE 5 CORRELATION FACTOR K_l FOR SLATS IN PRESENCE OF TRAILING-EDGE SLOTTED FLAPS

THE PREPARATION OF THIS DATA ITEM

The work on this particular Item was monitored and guided by the Aerodynamics Committee which first met in 1942 and now has the following membership:

Chairman

Mr H.C. Garner	–	Independent

Members

Mr G.E. Bean*	–	Boeing Commercial Airplane Co., Seattle, Wash., USA
Dr N.T. Birch	–	Rolls-Royce plc, Derby
Dr P.C. Dexter	–	British Aerospace plc, Sowerby Research Centre, Bristol
Mr J.R.J. Dovey	–	Independent
Dr K.P. Garry	–	Cranfield University
Mr D. Graham*	–	Northrop Grumman Corp., Pico Rivera, Calif., USA
Mr M.J. Green	–	Avro International Aerospace Ltd, Woodford
Dr H.P. Horton	–	Queen Mary and Westfield College, University of London
Dr D.W. Hurst	–	University of Southampton
Mr P.K. Jones	–	Independent
Mr K. Karling*	–	Saab-Scania AB, Linköping, Sweden
Mr M. Maurel	–	Aérospatiale, Toulouse, France
Mr C.M. Newbold	–	Aircraft Research Association, Bedford
Mr J.B. Newton	–	British Aerospace Defence Ltd, Warton
Mr R. Sanderson	–	Daimler-Benz Aerospace Airbus GmbH, Bremen, Germany
Mr A.E. Sewell*	–	McDonnell Douglas Corp., Long Beach, Calif., USA
Mr M.R. Smith	–	British Aerospace Airbus Ltd, Bristol
Mr J. Tweedie	–	Short Brothers plc, Belfast.

* Corresponding Member

The technical work in the assessment of the available information and the construction and subsequent development of the Data Item was carried out under contract by Mr J.R.J. Dovey.